Jet-Supercavity Interaction: Insights from CFD

M Kinzel[1], M Moeny[1], M Krane[1], and I Kirschner[2]
[1] Applied Research Laboratory, The Pennsylvania State University, University Park, PA, USA
[2] Applied Physical Sciences, Groton, CT, USA
E-mail: mpk176@psu.edu

Abstract. In this work, the interaction between a ventilated supercavity and a jet are examined using computational fluid dynamics (CFD). The CFD model is validated using experimental data, and shows to capture the correct trend in the bulk cavity behavior (qualitatively and quantitatively). Using these models, a number of novel insights into the physical characteristics of the interaction are developed. These interactions are described by: (1) the jet gas and ventilation gas poorly mix within the cavity, (2) the jet appears to cause additional gas leakage by transitioning the cavity from a recirculating flow to an axial flow, (3) the jet has the ability to lengthen the cavity, and (4) the jet invokes wake instabilities that drive cavity pulsation. These phenomena are documented and discussed in the following paper.

1. Introduction

Supercavitating vehicles operate within a supercavity that completely surrounds the vehicle in a gas to reduce skin friction. This is a concept that reduces power for high-speed underwater vehicles and mitigates adverse cavitation issues at high speed. Supercavitating vehicles often use ventilation gas to develop this cavity. Such cavities have been explored in detail without the coupling to propulsors.

A relatively unstudied interaction is that between a supercavity and a jet. Such an interaction is important when jets, or rockets, are used for propulsion. Previous studies in this topic are limited, and the work Paryshev [1] appears to be the most developed. Therein, the cavity-jet interaction was postulated to be dependent on the total pressure of the jet. When the total pressure of the jet is less than the free-stream total pressure of the liquid, the jet is relatively weak and acts to ventilate the cavity. On the contrary, as the total pressure of the jet increases above the total pressure in the liquid, the jet penetrates the cavity and increases gas leakage. Experimental observations tend to corroborate the theory [1].

This paper explores jets interacting with supercavities using CFD. The paper is organized as follows. A brief discussion of the experimental and numerical model setup is developed, which is followed by a benchmarking process. Results from the CFD model are then presented. This is followed by an interpretation of the solutions to provide new insight into cavity-jet interactions.

2. Methods

A validation effort is performed using a recent test campaign of cavity-jet interactions. Tests were performed in the 1.22m Garfield Thomas Water Tunnel at The Pennsylvania State University - Applied Research Laboratory [2]. The model consists of a sting-mounted, 30 deg, conical-shape cavitator (Fig. 1). A body extended from the cavitator to support a jet.

The CFD model is based on a three phase Eulerian multiphase model within Star-CCM+ [3]. The model uses 2nd-order differencing (space/time), along with a volume of fluid method using High-Resolution

Interface Capturing (HRIC) for the phase-conservation convection terms. The model uses incompressible liquid and isothermal compressible ventilation gas and jet gases. In these efforts, we use the improved delayed detached eddy simulation (IDDES) turbulence model [4], which is consistent with modeling requirements established by Kinzel et al. [5]. All cases are run on a series of four mesh/time resolutions to ensure mesh/time asymptotic solutions, with a fine-mesh solution using roughly 3.8×10^6 hex-dominant, unstructured volumes. The validation effort indicated that the prediction is within the uncertainty of the experiment for nearly all conditions. The CFD domain represents the experiment and is shown in Fig. 1, which focuses on results for a 11mm diameter jet at 13.7 m/s. Boundary conditions are applied as follows: (1) the upstream boundary inlet is 1.22" upstream of the vehicle, (2) the outlet is 3.8m downstream of the vehicle, (3) slip walls are used to represent the test-section walls, (4) no-slip walls are used to represent the sting, cavitator, and body (as shown in the blow up in Fig. 1), (5) ventilation ports are just downstream of the cavitator, and (6) a jet gas inlet through a converging nozzle that exits through the aft-end of the body.

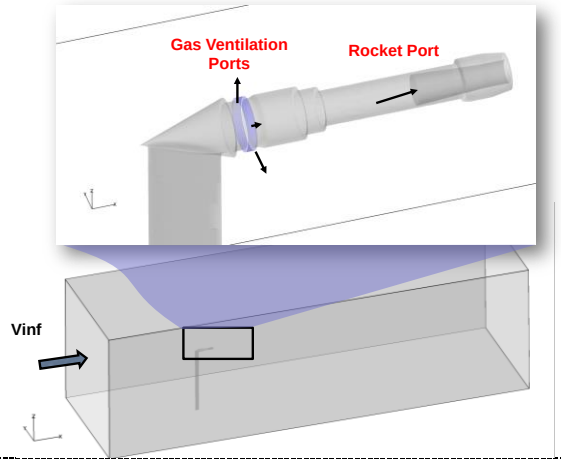

Figure 1. Diagram of the computational domain used to represent the experimental setup.

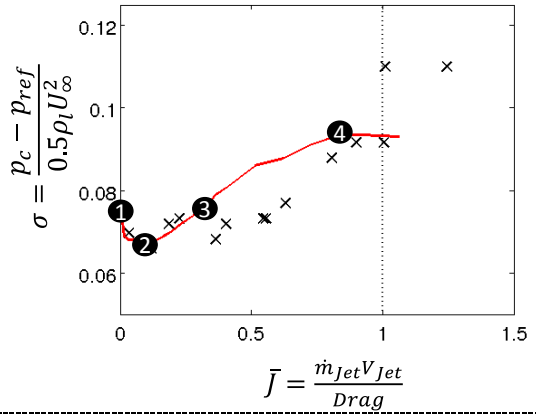

Figure 2. Benchmark of computational predictions (red line) as compared to the experimental measurements (X's).

3. Results

First, we review the validation of the CFD. Results from the studies are provided in Fig. 2 in the form of plots of σ_c versus $\bar{J}$. Cavitation number, $\sigma_c = \frac{(p_c - p_\infty)}{0.5\rho_l U_\infty^2}$, relates to cavity size and $\bar{J}$, $\bar{J} = \frac{(\dot{m}_{Jet} V_{Jet})}{Drag}$, is similar to the thrust-to-drag ratio (introduced by Paryshev [1]). Note that p_c is the cavity pressure, p_∞ is the free stream pressure, ρ_l is the liquid density, U_∞ is the free stream speed, $\dot{m}_{Jet}$ is the jet mass flow, V_{Jet} is the jet velocity, and *Drag* is the cavitator drag. For a $\bar{J}$ value of 0, there is no jet. As the jet is increases to a value of 1.0, thrust approximates self propulsion. And, for values greater than 1.0, the jet accelerates the vehicle. The CFD predictions (red line), predicted a range of conditions. The CFD and experiments indicate a similar trend and corroborate Paryshev [1]. This trend is defined as follows. Starting from a $\bar{J} = 0.0$, there is an initial drop in σ_c with increasing $\bar{J}$ until a $\bar{J}$ value of 0.3. Thereafter, σ_c increases with an increasing jet strength. In addition, the CFD predictions are in reasonable correlation with the experiments. With this, it is the opinion of the authors that the CFD is predicting the physical aspects of the interactions quite well and it is believed that insight from the CFD is relevant.

Flow visualization from the CFD results is provided in Fig. 3, which has four subfigures indicating:

(a) A representation of cavity shape (cyan-colored isosurface at a liquid volume fraction of 0.5) along with a corresponding pressure field contour plot on the center plane.
(b) Contour plot of the cavity ventilation gas indicating ventilation and jet gas mixing.

(c) The local air entrainment from the cavity as indicated by local air entrainment rate parameter, $C_{Q,loc}$, ($C_{Q,loc} = u/U_\infty \alpha_G$, where α_G is the gas volume fraction and u is the axial velocity). Positive values are plotted such that red indicates gas traversing from the cavity and blue indicates recirculating gas.
(d) The ratio of the local stagnation pressure to that in the free stream, plotted within the cavity. Red values indicate the gas has stagnation pressure equivalent to the liquid, blue indicates a weak jet. Note that stagnation pressure, p_0, is given as $0.5\rho U^2 + p$.

Each subfigure represents solutions from different conditions. These solutions are numbered (in the top-left corner), and correspond to the numbered points on the CFD solution results in Fig. 2. These results evaluate the solution at various regimes of the cavity-jet interaction.

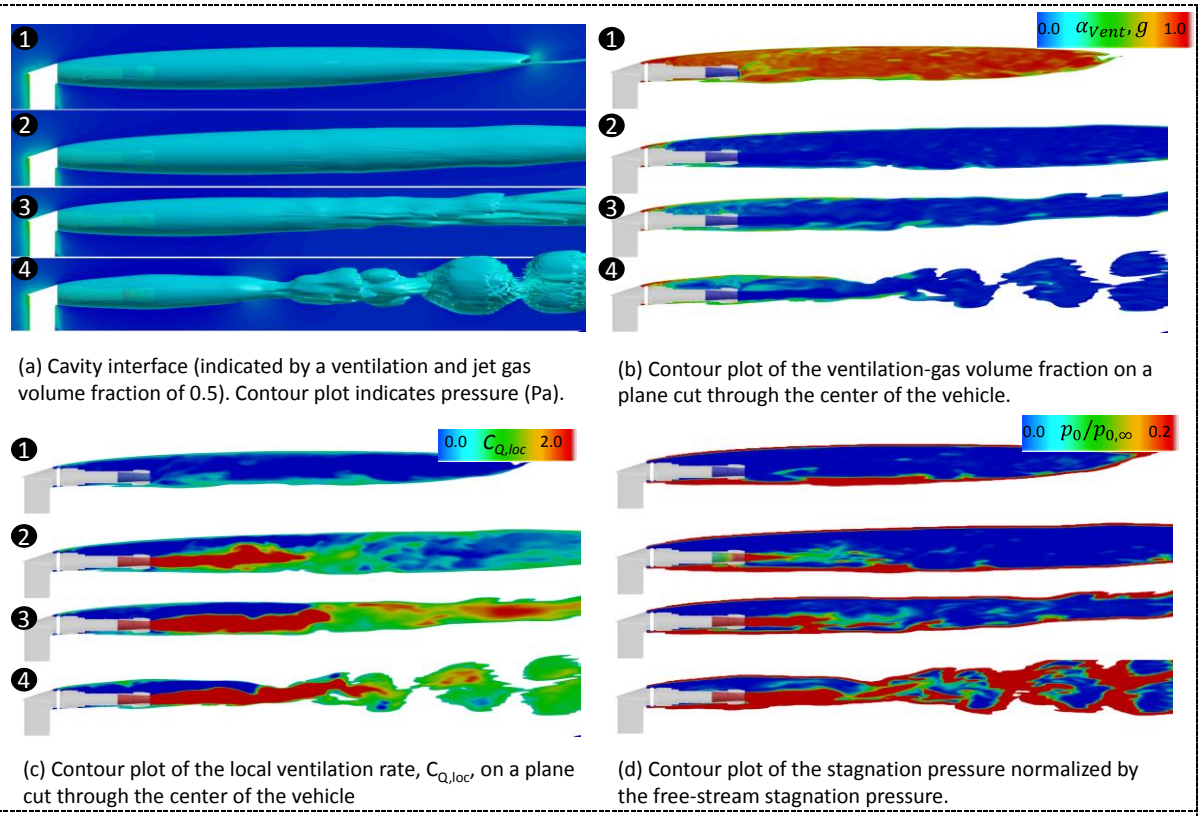

(a) Cavity interface (indicated by a ventilation and jet gas volume fraction of 0.5). Contour plot indicates pressure (Pa).

(b) Contour plot of the ventilation-gas volume fraction on a plane cut through the center of the vehicle.

(c) Contour plot of the local ventilation rate, $C_{Q,loc}$, on a plane cut through the center of the vehicle

(d) Contour plot of the stagnation pressure normalized by the free-stream stagnation pressure.

Figure 3. Flow field predictions. These plots are shown for four values of $\bar{J}$, corresponding to the numbered points in Fig. 2.

4. Discussion

4.1. Impact of Jet on the Cavity Shape

First, consider the cavity character with increasing jet strength (or $\bar{J}$). As indicated in Fig. 2, as the jet activates, σ_c sharply drops indicating the jets acts to ventilate. This is apparent in comparing the cavity sizes of the $\bar{J}$=0.0 and $\bar{J}$=0.11 cases in Fig. 3 (a), where the $\bar{J}$=0.11 case has a much larger cavity (note that cavity size ~ $1/\sigma_c$). As $\bar{J}$ increases to 0.37, the cavity diameter approaches the $\bar{J}$=0.0 case (note that σ_c values are similar), but the cavity length approaches that of the $\bar{J}$=0.11 case. This longer cavity for $\bar{J}$=0.37 is a difference and, as suggested by Paryshev [1], shows that the jet has the ability to lengthen the cavity for a given σ_c value. Lastly, for $\bar{J}$=0.84, a highly unsteady wake forms, and, as observed in animations, induces a pulsating cavity. In Fig. 3 (d), is the predicted $p_0/p_{0,\infty}$. The model of Paryshev [1] imposes a jet without decreases in p_0. CFD suggests the expansion process leads to rapid loss in p_0, and that the jet affects the cavity through different mechanisms.

4.2. Impact of Jet on the Cavity-Gas Composition

The next observation focuses on the gas content within the cavity. The behavior is shown in Figs. 3 (b), indicating that, an active jet dominates the gas within the cavity. The ventilation gas adheres to the cavity shear layers, as suggested by Spurk [7] and Kinzel et al. [8], and weakly mixes with the jet gas.

4.3. Impact of Jet on the Cavity-Gas Entrainment Mechanisms

Gas entrainment from the cavity is depicted in Fig. 3 (c). For the low $\bar{J}$ values, 0.0 and 0.11, gas moving out, shown by the non-blue $C_{Q,loc}$ regions, is dominated by cavity interface regions and the jet. With the weak jet ($\bar{J}$=0.11), the red shows the diffusing jet, with a blue region above the jet indicating that the recirculation process within the cavity is not disrupted. As $\bar{J}$ increases (to 0.37), the jet disrupts the re-circulatory region (when the cavity interface is scarred by the jet in Fig. 3 (a)). Aft of this point, is a transition from re-circulatory flow to axial flow. This axial flow appears to enable a more slender cavity. For $\bar{J}$=0.84, the re-circulatory region shortens and also develops into y axial flow. The difference in this condition, is that the axial flow region drives an oscillatory wake that could be driving cavity pulsation.

5. Summary and Conclusions

CFD simulations of cavity-jet interactions were performed and based on a new experimental data set. The CFD simulations tracked liquid, ventilation gas, and jet gas within the context of a IDDES simulation methodology. The CFD model was validated and found to be in reasonable agreement with experiment in terms of the correct trend and quantitative values. These simulation results are used to describe the physical characteristics of the cavity-jet interaction.

The cavity-jet interaction are defined as cavity size, character, gas composition, and gas entrainment. A regime of the jet acting to ventilate the cavity was observed, followed by a transition to the jet enhancing air entrainment. Observations indicated that re-circulatory cavity was altered by the jet and drives this breakdown process. For weak jets, where the jet was a ventilator, the re-circulatory process within the cavity was not disrupted. As the jet increased in strength, the re-circulatory flow was disrupted, and an axial cavity flow is developed leading to increased gas entrainment and cavity instabilities. This appears to dominate the cavity-jet interaction, which is not described in prior work. These fundamental processes observed within the CFD indicate new insight into the interaction of a jet with a supercavity.

6. Acknowledgments

Funding provided through ONR under contracts #N00014-13-1-0692 and #N00014-12-1-0489, with Dr. Ronald Joslin as the program manager.

7. References

[1] Paryshev E 2006 Approximate mathematical models in high-speed hydrodynamics *J. Eng. Math.* **55** 41–64
[2] Moeny M, Krane M, Kirschner I and Kinzel M 2015 Jet-Supercavity Interaction: Insights from Experiment *9th International Symposium on Cavitation (CAV2015)* (Lausanne, Switzerland)
[3] CD-Adapco 2014 Star-CCM+ 9.06
[4] Shur M L, Spalart P R, Strelets M K and Travin A K 2008 A hybrid RANS-LES approach with delayed-DES and wall-modelled LES capabilities *Int. J. Heat Fluid Flow* **29** 1638–49
[5] Kinzel M, Lindau J, Peltier L, Kunz R and Sankaran V 2007 Detached-Eddy Simulations for Cavitating Flows *18th AIAA Computational Fluid Dynamics Conference* Fluid Dynamics and Co-located Conferences (AIAA)
[6] Kinzel M P, Moeny M, Krane M, Kirschner I and Lindau J W 2015 A V&V Approach for a Parametric Investigation of Jet-Cavity Interactions for Supercavitation *ASME V&V2015* (Las Vegas, NV, USA)
[7] Spurk J H 2002 On the gas loss from ventilated supercavities *Acta Mech.* **155** 125–35
[8] Kinzel M P, Lindau J W and Kunz R F 2009 Air entrainment mechanisms from artificial supercavities: insight based on numerical simulations *7th International Symposium on Cavitation (CAV2009)* pp 1–14